Journal of ELECTRONIC MATERIALS, Vol. 47, No. 8, 2018
https://doi.org/10.1007/s11664-018-6370-y

TOPICAL COLLECTION: ELECTRONIC MATERIALS FOR RENEWABLE ENERGY APPLICATIONS

Optical, Electrical, and Crystal Properties of TiO_2 Thin Films Grown by Atomic Layer Deposition on Silicon and Glass Substrates

I. KUPA,[1,4] Y. UNAL,[1] S.S. CETIN,[2] L. DURNA,[1] K. TOPALLI,[3] A.K. OKYAY,[4] and H. ATES[1,5]

1.—Department of Metallurgical and Materials Engineering, Faculty of Technology, Gazi University, 06500 Ankara, Turkey. 2.—Department of Physics, Faculty of Science, Gazi University, 06500 Ankara, Turkey. 3.—Tubitak Space Technologies Research Institute, Ankara, Turkey. 4.—Okyay Tech., Yenimahalle, Ankara, Turkey. 5.—e-mail: hates@gazi.edu.tr

TiO_2 thin films have been deposited on glass and Si(100) by atomic layer deposition (ALD) technique using tetrakis(diethylamido)titanium(IV) and water vapor as reactants. Thorough investigation of the properties of the TiO_2/glass and TiO_2/Si thin films was carried out, varying the deposition temperature in the range from 100°C to 250°C while keeping the number of reaction cycles fixed at 1000. Physical and material property analyses were performed to investigate optical and electrical properties, composition, structure, and morphology. TiO_2 films grown by ALD may represent promising materials for future applications in optoelectronic devices.

Key words: TiO_2, ALD, characterization, solar cell

INTRODUCTION

Atomic layer deposition is a unique technique to grow thin films with excellent uniformity, conformity, and thickness control down to atomic monolayer scale.[1] It can be implemented in scalable fluidized bed reactors to treat nanoparticle surfaces.[2] The ALD method utilizes self-limiting surface chemistry to achieve growth rates typically on the order of 1 Å/cycle, varying with chemistry and deposition conditions.[3] Under appropriate conditions, deposition can be limited to the number of functional groups on the surface.[4] Underexposure of either precursor can lead to nodule growth, or islanding, a stochastic process that underutilizes available surface nucleation sites. With increasing number of cycles, nodules tend to grow together such that an effective growth rate can be defined, which will necessarily be lower than growth rates for the proper ALD window for given ALD chemistry. Overexposure, however, does not increase precursor adsorption beyond the surface-saturated threshold value,[5] but increases manufacturing costs and process time.[6] Typical applications for ALD films include semiconductor devices such as high-dielectric-constant gate oxides in metal–oxide–semiconductor field-effect transistor (MOSFET) structures, copper diffusion barriers in backend interconnects, energy applications, as well as micro- and nanoelectromechanical systems (MEMS/NEMS).[7–9] Specifically, application of ALD in solar cell research has received increasing attention in recent years.[1]

TiO_2 thin films are used in a wide variety of applications including photovoltaic devices,[10,11] corrosion-resistant coatings,[12] photocatalytic applications,[13] water purification agents,[14] antifogging coatings,[15] superhydrophilic coatings,[16] as well as antibacterial,[17] antifungal,[18] and antialgal[19] surface treatments. Related to TiO_2 thin-film characteristics, performance and practical usability are highly dependent on good interfacial properties, such as the film–substrate adhesion of coatings.[20] There are several methods for deposition of TiO_2 thin films, such as sol–gel,[21] vacuum sputtering,[22] and hydrothermal[23,24] growth. The ALD technique

(Received November 30, 2017; accepted May 8, 2018; published online May 22, 2018)

offers unrivaled thickness control and uniformity compared with traditional TiO_2 deposition techniques.[25–31]

In the work presented herein, the physical properties of TiO_2 thin films grown by ALD technique were investigated. TiO_2 thin films were deposited on glass and Si(100) substrates. Tetrakis(diethylamido)titanium(IV) (TDMAT) 99.999% ($[(C_2H_5)_2N]_4Ti$) and water vapor were used as precursor gases. Comprehensive investigation on the properties of the TiO_2/glass and TiO_2/Si film was carried out, varying the deposition temperature in the range from 100°C to 250°C while keeping the number of reaction cycles fixed at 1000. Ultraviolet–visible (UV–Vis) spectroscopy and ellipsometry were used to determine optical properties of the grown films. X-ray diffraction (XRD) analysis and x-ray photoelectron spectroscopy (XPS) were used to determine physical properties of the grown films. Electrical properties were investigated based on device current–voltage measurements, supported by XPS and XRD analyses.

EXPERIMENTAL PROCEDURES

TiO_2 thin films were grown on 4-inch *p*-type (100) single-side-polished (SSP) silicon wafers with thickness of 525 ± 20 micrometers and standard glass slides (ca. 0.5 mm). Films were grown in an OkyayTechALD T4 reactor. The process pressure was about 450 mtorr with constant flow (20 sccm) of nitrogen (99.999% purity) through reactant lines as carrier gas. One full ALD cycle consisted of (1) 100 ms TDMAT pulse, (2) 10 s purge to remove unreacted species, (3) 15 ms H_2O pulse, and (4) 10 s purge.

Si wafers were cleaned using acetone, alcohol, and deionized water to remove organic contaminants. The ALD chamber was preheated to 200°C. After cleaning, the wafer was immediately loaded into the reaction chamber. TDMAT has low vapor pressure at room temperature. To increase the TDMAT vapor pressure, the precursor bottle was heated to 75°C. A growth rate of 0.4 Å/cycle was calculated from optical measurements.

RESULTS AND DISCUSSION

AFM measurements revealed that the growth rate was slightly higher on silicon than glass substrates. This is mainly attributed to the higher tendency of the surface of the silicon substrate to adsorb water molecules. XRD results showed that thin films grown on silicon substrates had higher level of crystallinity compared with those grown on glass substrates. This difference in crystallinity is believed to be related to the crystallinity of the starting substrate. Silicon wafer is single crystalline, whereas glass substrate is amorphous. On a single-crystalline substrate such as silicon, the first few cycles result in larger grains, while films grow amorphous on glass substrate.

Electrical measurements on grown TiO_2 films showed that those grown on silicon exhibited higher electron mobility compared with those grown on glass substrate. However, the electron concentration was higher for the case of TiO_2 layer fabricated on glass substrate. This is mainly attributed to increased oxygen defects inside the bulk of the TiO_2 layer. As explained above, the film made on glass showed smaller grain size with overall crystallinity close to amorphous, while TiO_2 grown on Si exhibited polycrystalline nature with significantly larger grain boundaries. In general, formation of a larger number of grains increases the probability of electron recombination. Consequently, the electron mean free path is shorter, which results in lower electron mobility. However, these grains are proper sites for adsorption of chemisorbed oxygen groups. These oxygen radicals attach to the surface and release their electron to the bulk material. Therefore, films grown on glass substrate have higher carrier concentration. Furthermore, it was reported earlier that anatase crystal phase has significantly higher electron mobility compared with rutile phase of TiO_2. Our analysis also shows that, depending on the growth and sintering conditions, the phase mix in TiO_2 films can be tailored. This approach can be used to engineer the electron mobility by controlling the anatase/rutile phase in TiO_2 films.

Another property that defines the overall performance of the layer is its optical behavior. The optical behavior of the two films was therefore also compared. UV–Vis–near infrared (NIR) spectroscopy was performed on the samples to understand the absorption capability of both structures. Based on the obtained results, the film grown on silicon substrate showed quite similar absorption property compared with that grown on glass substrate. This is expected considering the fact that formation of oxygen deficiencies does not impact on the light absorption capability of the design but only its transport properties.

The phase structure of the obtained samples was identified using a PANalytical (X'Pert PRO MPD) instrument. The XRD patterns were collected over the 2θ angle range from 10° to 80° in Bragg–Brentano geometry (with Cu K_α source, primary and secondary Soller slits, 0.1 mm divergence slits, 0.3 mm receiving slit, and secondary graphite monochromator). Rietveld refinement of the XRD data was carried out using the TiO_2 structure to measure the amount of anatase and rutile phase.[32]

The surface chemical composition of the TiO_2 films was monitored by x-ray photoelectron spectroscopy (XPS) measurements, performed with a Thermo device in vacuum of 3×10^{-9} Torr (K_α-monochromated high-performance XPS spectrometer).

Figure 1 presents the XRD results for the TiO_2 films after sintering at different temperatures. All diffraction peaks could be indexed to anatase or rutile phase of TiO_2.

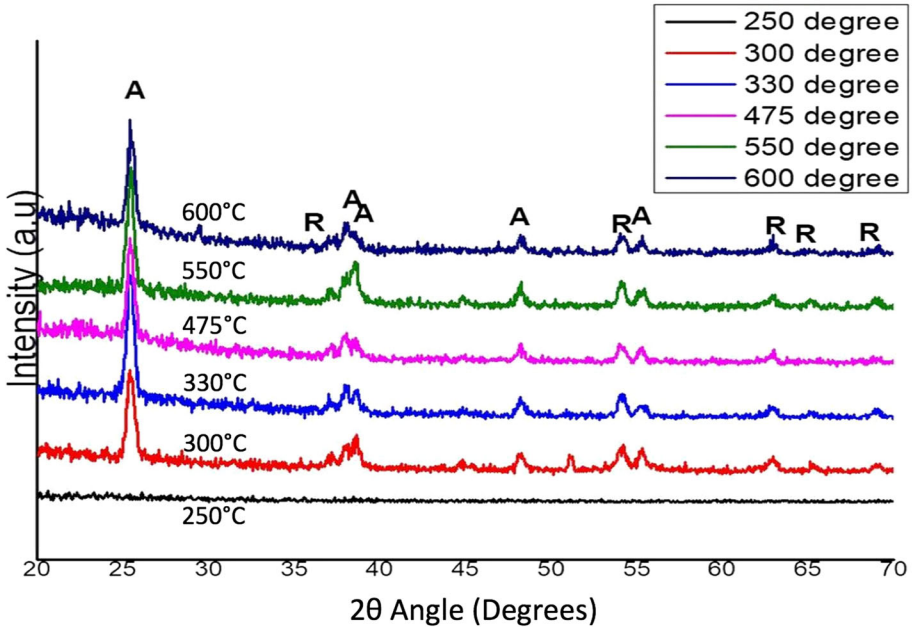

Fig. 1. XRD patterns of TiO_2 films after sintering at different temperatures.

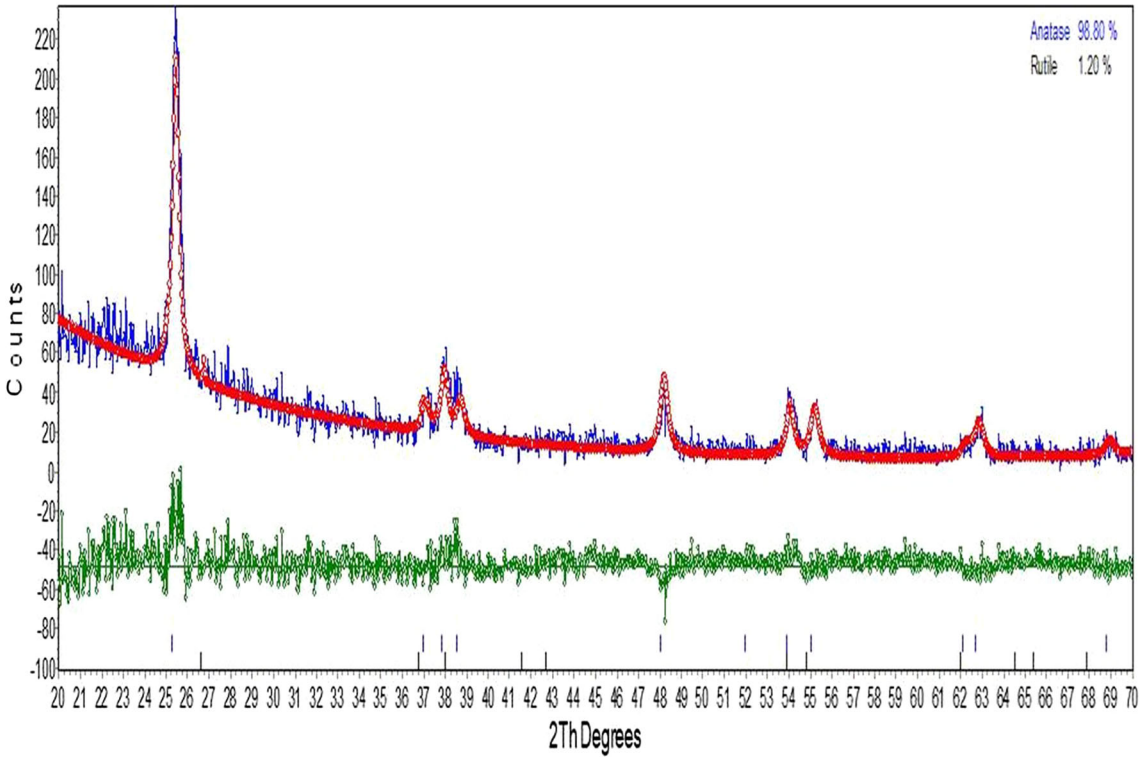

Fig. 2. Rietveld pattern determined from x-ray powder diffraction data for TiO_2.

Figure 2 shows the Rietveld pattern determined from x-ray powder diffraction data for TiO_2 film sintered at 475°C for 1 h. The plots denote the observed data, while the red line denotes the calculated profiles, and the green line denotes the difference. Vertical lines indicate possible Bragg peaks of TiO_2 phase.

Table I summarizes the anatase and rutile phase contents obtained by Rietveld quantitative analysis for TiO_2 films after sintering at different temperatures.

The surface composition of the TiO_2 films was characterized by XPS technique. The data analysis involved spectra normalization, Shirley background subtraction, and curve-fitting with Gaussian–Lorentzian (30% Lorentzian) line shape.[33] The best fits were determined using a root-mean-square measure with line shape, peak width (full-width at half-maximum, FWHM), and binding energy as adjustable parameters. Shirley backgrounds were used in all fits to narrow-scan spectra.[34]

The XPS survey-scan spectrum of the TiO_2 films is shown in Fig. 3a. All the XPS peaks were fit using Thermo Scientific Avantage software. Theory requires that O 1*s* and C 1*s* spectral lines consist of a single peak (singlet), whereas the Ti 2*p* spectrum consists of two peaks (spin–orbit doublet). The C 1*s* spectral line was standardized to 285.0 eV, and the O1*s* and Ti 2*p* spectra were adjusted to this energy.

Table I. Anatase and rutile phase contents (%) in TiO_2

Sintering temp. (°C)	Anatase	Rutile
300	73.56	26.44
330	84.99	15.01
475	98.81	1.19
550	88.21	11.79
600	96.42	3.58

Table II. Atomic concentrations calculated from XPS results for TiO_2 films

Sintering temperature	Atomic percentage (%) from peak regions			O–H/Ti–O ratio
	530.31	531.84	532.94	
300	11.28	3.4	–	0.301
330	10.1	4.85	–	0.480
400	9.64	4.92	–	0.510
475	7.08	5.56	–	0.785
550	6.75	3.11	2.24	0.461
600	9.26	4.57	–	0.494

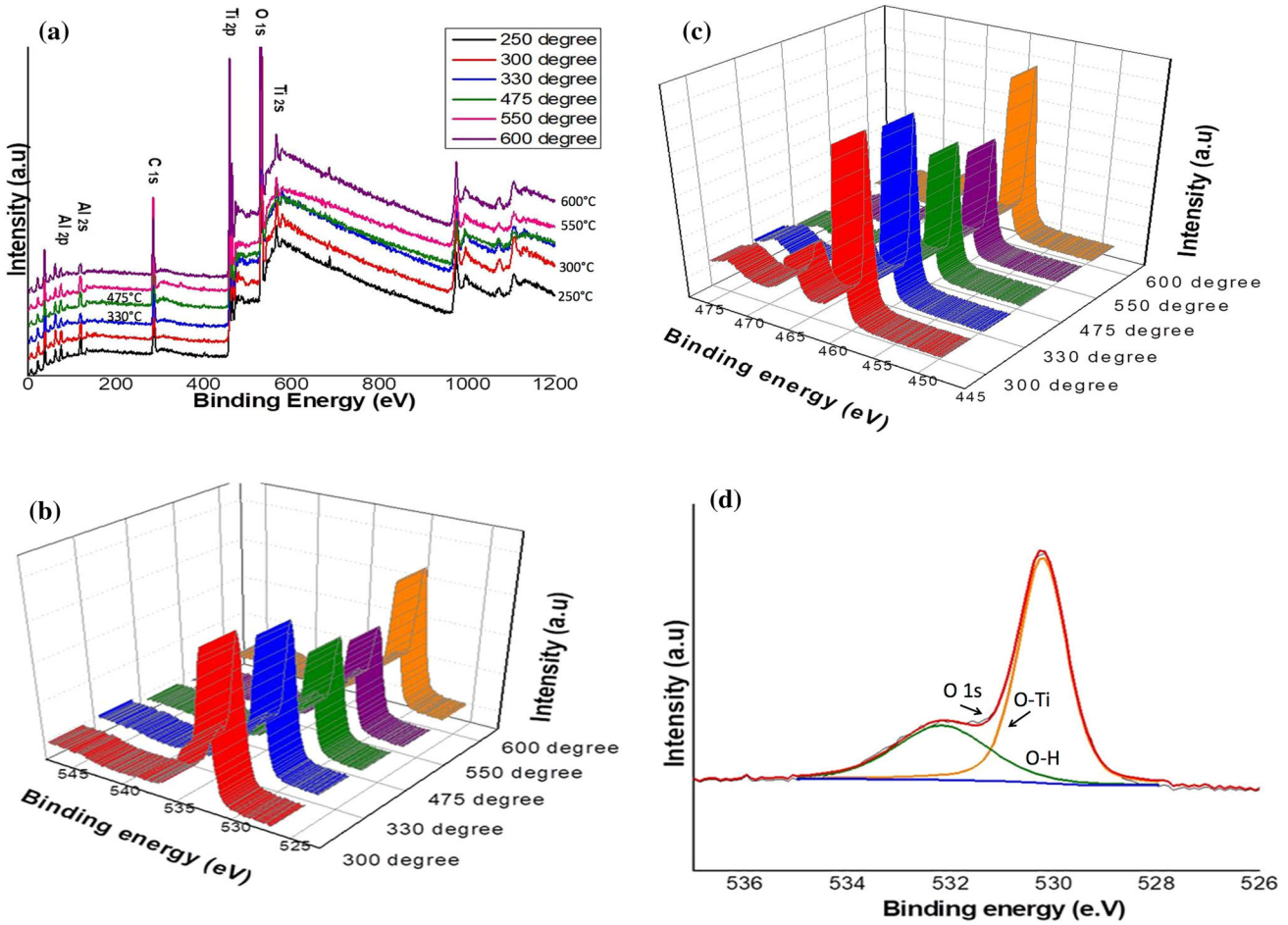

Fig. 3. (a) Wide-scan survey XPS spectrum of TiO_2 film, (b) XPS spectrum in O 1*s* region, (c) XPS spectrum in Ti 2*p* region, and (d) narrow scan of O 1.

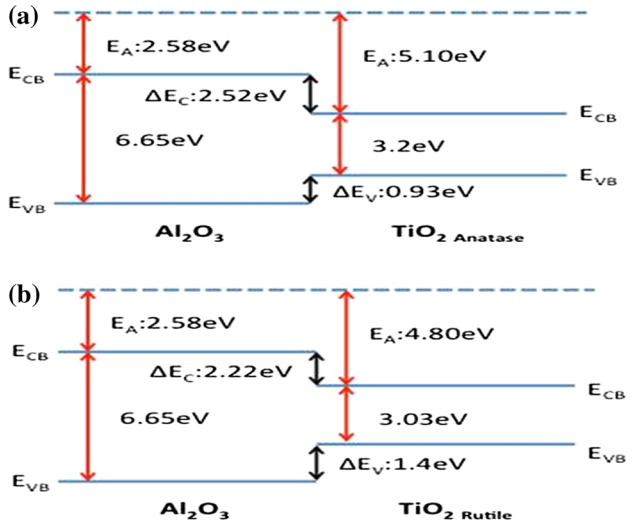

Fig. 4. Energy band diagram and alignment offsets for alumina–titania junction: (a) anatase TiO_2 and (b) rutile TiO_2.

The O 1*s* spectrum of TiO_2 film can be deconvoluted into two peaks, one at 530.2 eV and another at 531.84 eV. However, the O 1*s* spectrum of the obtained TiO_2 film sintered at 575°C could be resolved into three peaks, one at 530.2 eV, and another two at 531.84 eV and 532.4 eV, respectively. Based on literature, the main peak at 530.2 eV is due to the oxygen lattice and Ti–O bond, while the peak at 531.2 eV corresponds to water (O–H) and hydroxide absorbed on the surface and the peak at 532.9 eV is probably due to water and hydroxide Ti or basic OH on the surface.[35–41] Table II summarizes the atomic percentage for the samples and the O–H/Ti–O ratio.

Figure 4 depicts calculated energy band diagrams for anatase and rutile TiO_2 with alignment offsets with Al_2O_3 obtained from literature. Alumina–titania junctions are very common in electrical device applications such as thin-film MOS transistors, where alumina is the gate oxide.[42]

Optical characterization of the ALD-grown TiO_2 films was performed to obtain their spectral transmission using the UV–VIS–NIR technique, and the optical bandgap using the photoluminescence technique. Figure 5a shows transmission versus wavelength for 50-nm-thick ALD TiO_2 film deposited on quartz (chosen instead of glass to avoid background absorption due to the substrate at these wavelengths). The strong peak observed at 360 nm ($\sim$ 3.4 eV) is close to reported values for direct-bandgap energies for anatase-phase (3.3 eV) TiO_2. Figure 5b shows photoluminescence spectra of 50-nm-thick ALD TiO_2 film deposited on quartz substrate. A significant drop in transmission is observed at UV wavelengths lower than 375 nm, in agreement with main direct-bandgap optical absorption.

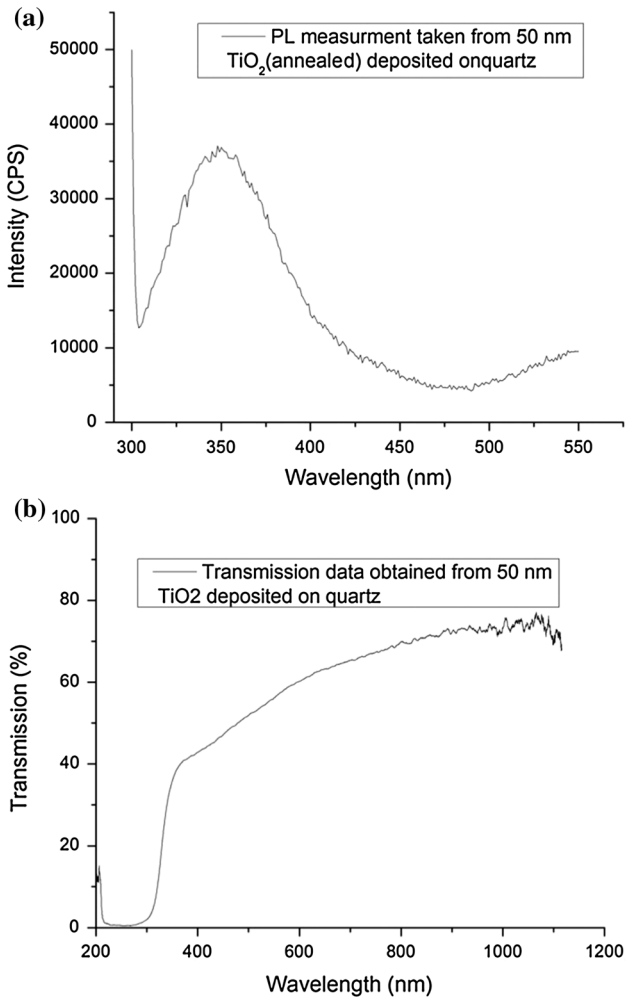

Fig. 5. (a) Transmission versus wavelength and (b) spectral photoluminescence of 50-nm-thick ALD TiO_2 film deposited on quartz.

CONCLUSIONS

Comprehensive study was carried out on the impact of substrate type on the structural, electrical, and optical properties of ALD-grown TiO_2 film. The results demonstrate that formation of defects is more likely in the case of glass substrate, which could negatively affect the electrical properties of ALD TiO_2 film. It can be concluded that the choice of substrate could provide an option to control the electrical properties of such layers.

ACKNOWLEDGEMENT

The authors would like to thank Gazi University Projects 07/2015-08 and 07/2016-11 for support.

REFERENCES

1. W. Chiappim, G.E. Testoni, R.S. Moraes, R.S. Pessoa, J.C. Sagas, F.D. Origo, L. Vieira, and H.S. Maciel, *Vacuum* 123, 91 (2016).
2. C.S. Kovash Jr., J.D. Hoefelmeyer, and B.A. Logue, *Electrochim. Acta* 67, 18 (2012).

3. P.J. Cameron and L.M. Peter, *J. Phys. Chem. B* 109, 7392 (2005).
4. T.W. Hamann, A.B.F. Martinson, J.W. Elam, M.J. Pellin, and J.T. Hupp, *J. Phys. Chem. C* 112, 10303 (2008).
5. D.H. Kim, M. Woodroof, K. Lee, and G.N. Parsons, *ChemSusChem* 6, 1014 (2013).
6. D.M. King, X. Liang, Y. Zhou, C.S. Carney, L.F. Hakim, P. Li, and A.W. Weimer, *Powder Technol.* 183, 356 (2008).
7. S.M. George, *Chem. Rev.* 110, 111 (2010).
8. M. Ritala and J. Niinistö, *ECS Trans.* 25, 641 (2009).
9. C.-T. Wang and H.-L. Siao, *Surf. Coat. Technol.* 244, 63 (2014).
10. T.-T. Duong, Y.-J. Kim, J.-H. Eom, J.-S. Choi, A.-T. Le, and S.-G. Yoon, *RSC Adv.* 5, 33515 (2015).
11. E. Marin, A. Lanzutti, M. Lekka, L. Guzman, W. Ensinger, and L. Fedrizzi, *Surf. Coat. Technol.* 211, 84 (2012).
12. H. Yaghoubi, N. Taghavinia, and E.K. Alamdari, *Surf. Coat. Technol.* 204, 1562 (2010).
13. A. Ghobadi, T.G. Ulusoy, R. Garifullin, M.O. Guler, and A.K. Okyay, *Sci. Rep.* 6, 30587 (2016).
14. W.S. Law, S.W. Lam, W.Y. Gan, J. Scott, and R. Amal, *Thin Solid Films* 517, 5425 (2009).
15. S. Zhuiykov, M.K. Akbari, Z. Hai, C. Xue, H. Xu, and H. Lachlan, *Mater. Des.* 120, 99 (2017).
16. Y. Xiong, M. Lai, J. Li, H. Yong, H. Qian, C. Xu, K. Zhong, and S. Xiao, *Surf. Coat. Technol.* 265, 78 (2015).
17. C.C. Trapalis, P. Keivanidis, G. Kordas, M. Zaharescu, M. Crisan, A. Szatvanyi, and M. Gartner, *Thin Solid Films* 433, 186 (2003).
18. G. Kosarsoy, E.H. Sen, N. Aksoz, S. Ide, and H. Aksoy, *Appl. Surf. Sci.* 318, 269 (2014).
19. X. Wang, J. Zhang, W. Sun, W. Yang, J. Cao, Q. Li, Y. Peng, and J.K. Shang, *Chem. Eng. J.* 264, 437 (2015).
20. J. Lyytinen, X. Liu, O.M.E. Ylivaara, S. Sintonen, A. Iyer, S. Ali, J. Julin, H. Lipsanen, T. Sajavaara, R.L. Puurunen, and J. Koskinen, *Wear* 342–343, 270 (2015).
21. R.C. Suciu, E. Indrea, T.D. Silipas, S. Dreve, M.C. Rosu, V. Popescu, G. Popescu, and H.I. Nascu, *J. Phys: Conf. Ser.* 182, 012080 (2009).
22. J. Musil, D. Heřman, J. Šícha, *J. Vac. Sci. Technol. A Vac. Surf. Films* 24, 521 (2006).
23. M. Ghaffari, B. Cosar, H.I. Yavuz, M. Ozenbas, and A.K. Okyay, *Electrochim. Acta* 76, 446 (2012).
24. H. Karaagac, L.E. Aygun, M. Parlak, M. Ghaffari, N. Biyikli, and A.K. Okyay, *Phys. Status Solidi Rapid Res. Lett.* 6, 442 (2012).
25. J. Aarik, A. Aidla, T. Uustare, K. Kukli, V. Sammelselg, M. Ritala, and M. Leskela, *Appl. Surf. Sci.* 193, 277 (2002).
26. R. Garifullin, H. Eren, T.G. Ulusoy, A.K. Okyay, N. Biyikli, and M.O. Guler, *Phys. Status Solidi A* 213, 3238 (2016).
27. A. Haider, H. Cansizoglu, M.F. Cansizoglu, N. Biyikli, A.K. Okyay, and T. Karabacak, *J. Vac. Sci. Technol. A Vac. Surf. Films* 33, 01A110 (2015).
28. R. Hussin, K.L. Choy, and X.H. Hou, *Adv. Mater. Res.* 1133, 352 (2016).
29. C. Jin, B. Liu, Z. Lei, and J. Sun, *Nanoscale Res. Lett.* 10, 95 (2015).
30. Y.J. Shi, R.J. Zhang, H. Zheng, D.H. Li, W. Wei, X. Chen, Y. Sun, Y.F. Wei, H.L. Lu, N. Dai, and L.Y. Chen, *Nanoscale Res. Lett.* 12, 243 (2017).
31. Z.P. Yang, H.E. Cheng, I. Chang, and I.S. Yu, *Appl. Sci. J.* 6, 8 (2016).
32. L.B. McCusker, R.B. Von Dreele, D.E. Cox, D. Louer, and P. Scardi, *J. Appl. Crystallogr.* 32, 36 (1999).
33. V.P. Zakaznova-Herzog, H.W. Nesbitt, G.M. Bancroft, and J.S. Tse, *Surf. Sci.* 600, 3175 (2006).
34. D.A. Shirley, *Phys. Rev. B* 5, 4709 (1972).
35. J. Chastain, *Handbook of x-ray Photoelectron Spectroscopy* (Waltham: Perkin-Elmer, 1992).
36. V. Young and T. Otagawa, *Appl. Surf. Sci.* 20, 228 (1985).
37. D. Briggs and M.P. Seah, eds., *Surface and Interface Analysis* (Chichester: Wiley, 1983), p. xiv + 533.
38. C. Wagner, D. Zatko, and R. Raymond, *Anal. Chem.* 52, 1445 (1980).
39. S.J. Xiao, M. Textor, N.D. Spencer, and H. Sigrist, *Langmuir* 14, 5507 (1998).
40. C. Viornery, Y. Chevolot, D. Leonard, B.O. Aronsson, P. Pechy, H.J. Mathieu, P. Descouts, and M. Gratzel, *Langmuir* 18, 2582 (2002).
41. N.A. Smith, G.G. Antoun, A.B. Ellis, and W.C. Crone, *Compos. A Appl. Sci. Manuf.* 35, 1307 (2004).
42. A.K. Okyay, F.B. Oruç, F. Cimen, and L.E. Aygün, *Proc. SPIE Int. Soc. Opt. Eng.* 8626, 16 (2013).